Acetylcholinesterase Inhibitory Activity of Scopolin and Scopoletin Discovered by Virtual Screening of Natural Products†

Judith M. Rollinger,*,‡,§ Ariane Hornick,|| Thierry Langer,§,⊥ Hermann Stuppner,‡,§ and Helmut Prast||

Department of Pharmacognosy, Department of Pharmacology and Toxicology, and Department of Pharmaceutical Chemistry, Computer Aided Molecular Design Group, Institute of Pharmacy, Leopold-Franzens University of Innsbruck, A-6020 Innsbruck, Austria, and Inte:Ligand GmbH, Software-Engineering and Consulting, Clemens Maria Hofbauergasse 6, A-2344 Maria Enzersdorf, Austria

Received May 7, 2004

For the targeting selection of acetylcholinesterase (AChE) inhibitors from natural sources we generated a structure-based pharmacophore model utilizing an in silico filtering experiment for the discovery of promising candidates out of a 3D multiconformational database consisting of more than 110 000 natural products. In our study, scopoletin (**1**) and its glucoside scopolin (**2**) emerged as potential AChE inhibitors by the virtual screening procedure. They were isolated by different chromatographic methods from the medicinal plant *Scopolia carniolica* Jaqc. and tested in an enzyme assay using Ellman's reagent. They showed moderate, but significant, dose-dependent and long-lasting inhibitory activities. In the in vivo experiments (icv application of 2 μmol) **1** and **2** increased the extracellular acetylcholine (ACh) concentration in rat brain to about 170% and 300% compared to basal release, respectively. At the same concentration, the positive control galanthamine increased the ACh concentration to about the same level as **1**. These are the first in vivo results indicating an effect of coumarins on brain ACh.

Introduction

The potency of natural products to treat and cure human diseases is well-known and has been for living memory. Even today, in the century of combinatorial chemistry, secondary metabolites of plants, fungi, marine organisms, and microorganisms are still an important source for the development of new drugs.[1,2] About 50% of the drugs introduced to the market during the last 20 years are derived directly or indirectly from small molecules of natural origin.[1] Their potential has also been successfully demonstrated in the field of Alzheimer's disease (AD).[3,4] Although the aetiology of AD is still unknown, its neuropathological occurrence associated with memory loss is consistent with the presence of numerous plaques and a cholinergic deficiency due to the degeneration or atrophy of cholinergic neurons in the basal forebrain.[5] At present, the cholinesterase inhibition is the mainstay of treatment for AD and also serves as a promising strategy for the treatment of senile dementia, ataxia, myasthenia gravis, and Parkinson's disease. Acetylcholinesterase (AChE) inhibitory drugs increase the effectiveness of cholinergic transmissions by inhibiting the metabolic hydrolysis of acetylcholine.[6,7] In addition, evidence has been presented that AChE could also play a key role in accelerating amyloid β-peptide (Aβ) plaque deposition.[8,9] Since Aβ is the main component of the senile plaques found in the brain of AD patients, any compounds able to inhibit the plaque's aggregation might be regarded as potentially useful in the treatment of AD.

Within the wide range of natural products, physostigmine, an indolic alkaloid from the seeds of *Physostigma venenosum* BALFOUR, turned out to be one of the first principle anticholinesterases. However, it only shows a modest improvement in the cognitive function of Alzheimer's patients due to its poor brain penetration, oral bioavailability, and pharmacokinetic parameters.[7] Alkaloids of a number of Amaryllidaceae have been screened for AChE activity,[10] and one of the most potent of these emerged as galanthamine (GNT) from *Galanthus nivalis* L., which is now marked for the treatment of AD in Austria (Reminyl). The alkaloid is selective, long-acting, reversible, and produces beneficial cognitive effects in patients.[11] Despite the substantial progress, there is still a great interest in finding better AChE inhibitors to give faster penetration in the central nervous system (CNS), longer duration of action, and lower toxicity.

Despite the definite potential of some natural products to enhance the cholinergic function in the CNS by their anticholinesterase effect, there is still a problem associated with the targeting selection due to the multitude and chemical diversity of natural products. Our method to overcome this challenge consists of the application of modern computer-aided screening techniques such as pharmacophore modeling coupled together with virtual screening (VS). The potential of feature-based pharmacophore modeling as a screening tool for a successful 3D database search is widely accepted and has recently been reviewed.[12] However, it will only be efficient if enough structural information about the target, or compounds that bind to the target, are available to create a reliable pharmacophore model.

† European patent application number 04009431.0.

* Corresponding author. Phone: +43 512 507 5308. Fax: +43 512 508 2939. E-mail: judith.rollinger@uibk.ac.at.

‡ Department of Pharmacognosy, Leopold-Franzens University of Innsbruck.

§ Inte:Ligand GmbH.

|| Department of Pharmacology and Toxicology, Leopold-Franzens University of Innsbruck.

⊥ Department of Pharmaceutical Chemistry, Computer Aided Molecular Design Group, Leopold-Franzens University of Innsbruck.

10.1021/jm049655r CCC: $27.50
Published on Web 11/09/2004

Since 3D structure information of the complex structure of GNT and AChE is available, a pharmacophore model was generated and checked for its reliability. For the computer-aided approach we used our in-house 3D database, NPD, recently described by Rollinger and coauthors.[13] This consists of about 110 000 natural products within a molecular mass of 140−700 Da. On the basis of the obtained hits of the VS, we focused on scopoletin (**1**, 7-hydroxy-6-methoxycoumarin, SCT) and scopolin (**2**, 7-*O*-*β*-glucopyranoside-6-methoxycoumarin, SCN). These two coumarins widely occur as secondary plant metabolites, especially in a number of members of the Solanaceae family. SCT has previously been described as an anti-inflammatory[14,15] and antiproliferative agent[16] that exhibits activities such as the inhibition of inducible nitric oxide synthase and prostaglandin synthase.[17−19] Furthermore, it inhibits the monoamine oxidase at moderate concentrations[20] and may act as an antioxidant and a radical scavenger.[21,22]

The aim of this study was to demonstrate the strategy of utilizing computer-aided drug discovery in search for improved AChE inhibitors in the field of natural products. We therefore isolated SCT and SCN from *Scopolia carniolica* Jaqc. and undertook an exploratory study of their in vitro and in vivo AChE inhibitory effect.

Results and Discussion

Generation of the Pharmacophore Model for AChE Inhibitors. Virtual Screening. Pharmacophore models have often proven to be useful tools for rationalizing ligand−target interaction and for making this information available to VS techniques. Chemical function based pharmacophore models consist of a number of so-called "features" that are located relative to each other in coordinate space as points surrounded by a sphere of tolerance. Each sphere represents the region in space that should be occupied by a certain chemical functionality capable of the kind of interaction specified by the feature type. In organic molecules, different structural motifs can express the similar chemical behavior and therefore the same biological effect. The concept of feature-based pharmacophores is implemented in several software environments representing widely used platforms for VS. For this study the feature-based pharmacophore model was obtained starting from 3D structural information from a protein−ligand complex available as a PDB file,[23] using the LigandScout software package.[24]

The 3D structure of AChE has been known since the first X-ray crystal structures of *Torpedo californica* AChE in complex with tacrine and with edrophonium were described by Harel and co-workers in 1993.[25] The three-dimensional structure of the GNT−AChE complex was published by Bartolucci and coauthors.[26] This was used as the starting point for the generation of the pharmacophore model in the present study. The model exhibits four essential features, as represented in Figure 1: one H-bond-donor function (HBD) pointing from the GNT hydroxyl group to GLU-199, one H-bond-acceptor function (HBA) located at GNT's methoxy oxygen atom, and two hydrophobic features (HY) positioned on the aromatic ring and on the cyclohexene moiety of the ligand. Exclusion volume spheres are located in this model on the aromatic moieties of the surrounding amino acids Phe290, Phe330, Tyr121, and Trp84. To further restrict the 3D search space, a molecular shape constraint generated from the structure of GNT aligned with the pharmacophore model was added (Figure 2). The Cartesian coordinate triples for all the features of this pharmacophore model are listed in Table 1.

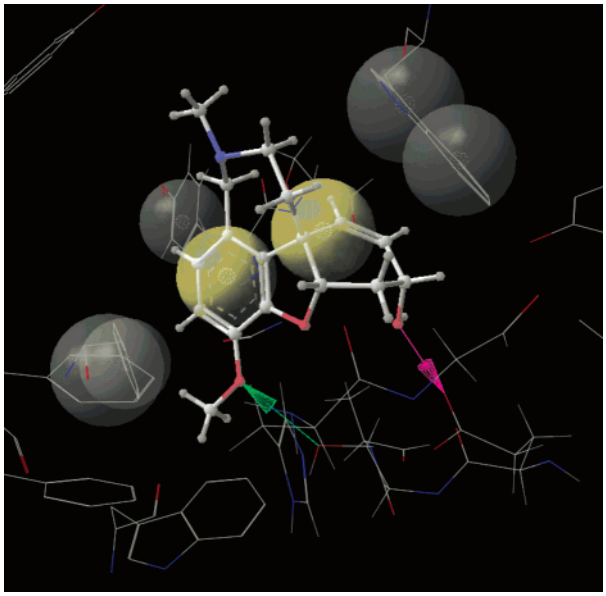

Figure 1. LigandScout pharmacophore model identified from GNT−AChE complex 1QTI (magenta arrow, HBD; green arrow, HBA; yellow spheres, HY; gray spheres, exclusion volume spheres).

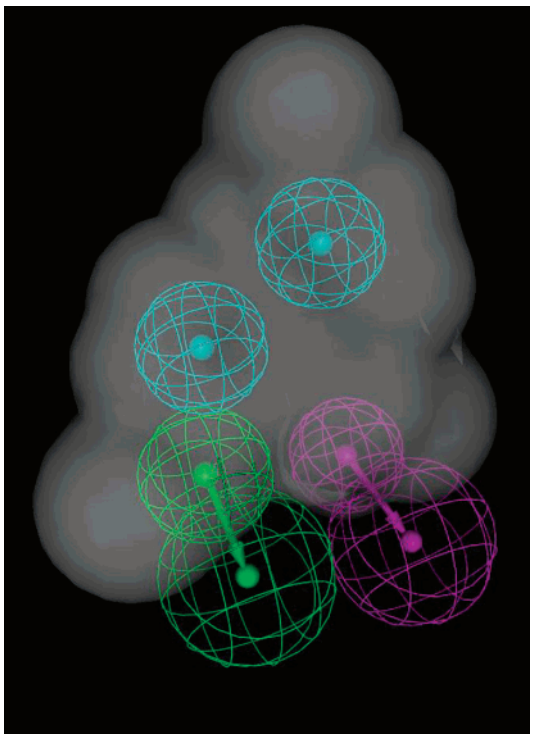

Figure 2. Pharmacophore model used within Catalyst for VS (magenta, HBD; green, HBA; blue, HY; gray volume area, molecular shape constraint).

On the basis of the hits obtained by the VS experiment, scopoletin (SCT, **1**) and particularly its glycoside scopolin (SCN, **2**) emerged as promising candidates (Figure 3).

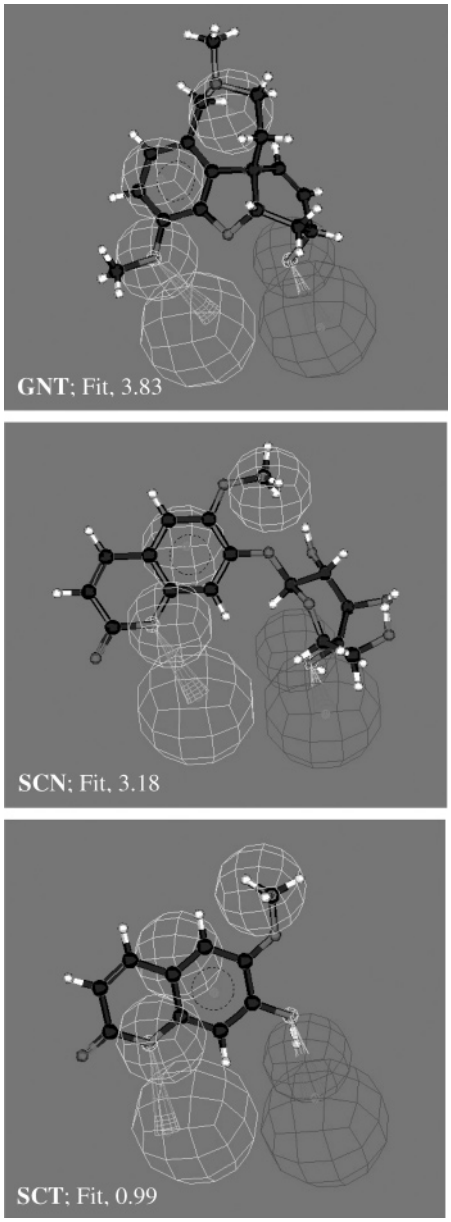

Figure 3. Possible mappings and corresponding fitting values of GNT, SCN, and SCT with the generated model used within Catalyst (arrangement of the features as in Figures 1 and 2).

Table 1. Cartesian Coordinates of the Elaborated Pharmacophore Model

feature	size (Å)	Cartesian coordinates (Å) X	Y	Z
hydrophobic	1.5	−11.952	6.978	−0.825
hydrophobic	1.5	−10.774	3.866	−2.252
HBA heavy atom	1.5	−8.899	7.534	−5.854
HBA projected point	2.0	−6.308	8.298	−6.185
HBD heavy atom	1.5	−8.258	3.255	−3.480
HBD projected point	2.0	−6.546	3.934	−5.810

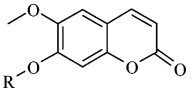

1 R = H (**SCT**)

2 R = b-D-Glucopyranose (**SCN**)

Due to their existence in the roots of *S. carniolica* Jacq. (Solanaceae),[27,28] we selected this perennial medicinal plant for the isolation of the targeted coumarins. According to the solubility of the comprising coumarins, a methanolic extract of the rhizomes of *S. carniolica* was produced and screened in a bioautographic TLC test in order to evaluate its AChE inhibitory activity. The fluorescent TLC spots at R_f 0.6 and 0.4, corresponding to SCT and SCN, respectively, emerged as positive. False positive results could be excluded by applying a TLC bioautographic assay as described by Rhee and coworkers.[29] Using different chromatographic methods, SCT and SCN were isolated and identified by TLC,[27] ^{1}H NMR,[28] and LC−MS.[30] The activity of the isolated compounds was quantitatively tested and compared to GNT in a microplate assay.[31] All three drugs inhibited AChE activity in a dose-dependent manner (Figure 4). The concentration of SCT required for half-maximal AChE inhibition (IC_{50}) was determined to be 168.6 μM (CI_{95} = 150.5−188.8). The IC_{50} obtained for GNT fits well to the data already described in the literature. Lopez and coauthors report an IC_{50} of 1.07 μM, using preincubation of the enzyme with GNT before adding Ellman's reagent.[32] Rhee and coauthors report an activity of about 50% at 2.5 μM.[10] In our assay, GNT exhibited an IC_{50} of 3.2 μM (CI_{95} 2.4−4.2). SCN, however, exerted an AChE inhibitory activity of 30.1% at 1000 μM ($p < 0.001$, measurement after 60 min). Although the inhibition for 1000, 500, and 250 μM proved to be significant, the IC_{50} of SCN was not determined because of its weak activity.

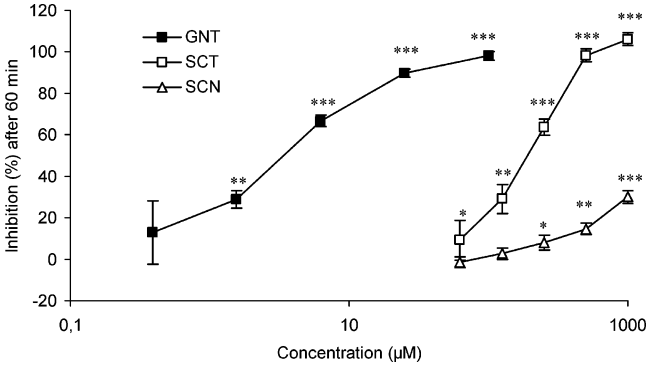

Figure 4. Microplate assay: inhibitory effect of different concentrations of GNT, SCT, and SCN on AChE. Statistical analysis: data are means ± SD; ***$p < 0.001$, **$p < 0.01$, *$p < 0.05$, Student's test of absorption data after 60 min in comparison with medium control, $n = 4$.

The in vitro inhibition of AChE caused by five different concentrations of SCT was measured over 90 min. The data (Figure 5) shows that at lower concentrations (62.5 and 125 μM) the level of inhibitory activity is reached within the first 15 min by adding the enzyme to the substrate and it lasts for at least 90 min. At higher concentrations of SCT (250, 500, and 1000 μM), a slight, almost insignificant increase in inhibitory activity is determined up to 90 min. In the case of SCN, the inhibitory activities of the three highest concentrations (Figure 5) reach their maximum extent within the first 15 min followed by a slight decrease toward the endpoint of measurement at 90 min. However, the inhibitory activity of SCN is 5.4×10^2 lower compared to that of GNT (calculated for 30% inhibition, measured after 60 min). The extent of AChE inhibition caused by GNT is constant within the time of measurement (Figure 5), indicating a competitive manner of inhibition as already described in the literature.[33]

In Vivo Extracellular Acetylcholine (ACh) Concentration. Furthermore, a goal was set to test the

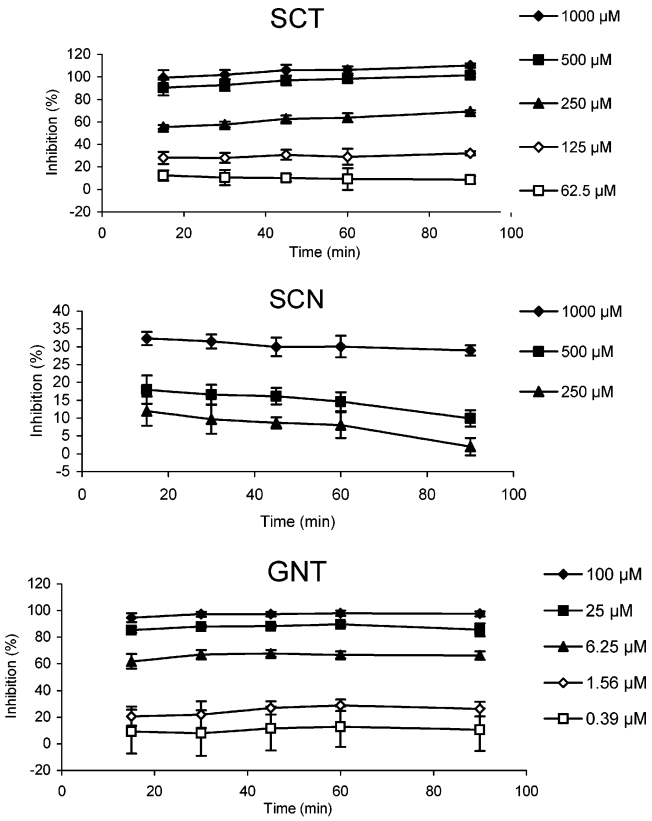

Figure 5. Microplate assay: time dependent inhibitory effect of different concentrations of SCT, SCN, and GNT in comparison with medium control. Data are means ± SD, $n = 4$.

compounds for their effectiveness in enhancing cholinergic transmission in the brain in vivo. For this purpose, we monitored the extracellular ACh concentration in the brain of rats with the push−pull technique and injected the putative inhibitors into the cerebral ventricle. In analogy to the in vitro experiments, the effect of GNT was observed as well in the in vivo study. Its effect on ACh in rat brain has not yet been previously investigated.

Basal Concentration and Injection of Vehicle. Sixty minutes after beginning the superfusion, the extracellular ACh concentration reached a stable level, which did not change throughout the experiment. The basal output of ACh in the nucleus accumbens of urethane-anaesthetized rat was 83.30 ± 10.82 fmol/min ($n = 39$). The icv injection of vehicles, DMSO−EtOH (1:1; Figure 6) and DMSO (not shown), did not significantly influence the basal concentration of ACh.

Administration of 1 and 2 μmol of GNT (Figure 6A,B) induced an increase in the extracellular concentration of ACh. Both doses caused an effect of similar magnitude (means ± SEM: 1.78 ± 0.32 and 1.68 ± 0.20). Although, in the group treated with the lower dose the effect of GNT showed a higher variability (Figure 6A).

Both coumarins induced a pronounced and long-lasting increase in the extracellular concentration of ACh. As shown in Figure 6C, the injection of SCT enhanced the concentration to a continuous level of about 1.7 times the basal value (mean ± SEM, 1.74 ± 0.24). In contrast to the results obtained from the in vitro experiments, the increase in ACh by the glucoside SCN was higher (mean ± SEM, 3.18 ± 0.78) and showed an initial peak concentration of about 400% of the basal value followed by a decline to about 200% (Figure 6D).

The data demonstrates that the values received from the in vitro examination alone were not indicative of the activity displayed in vivo. The reasons for this incoherence are not known and have to be further investigated. Perhaps, the higher effectiveness of SCN in vivo is due to pharmacokinetic properties such as a different rate of tissue distribution and/or metabolism that leads to a higher striatal concentration of the compound, compared to SCT. In the VS experiment, however, SCN clearly maps better to the pharmacophore hypothesis features than SCT (see Figure 3), exhibiting a fit value in the same range as GNT (SCN, 3.18; GNT, 3.83). Although we are aware that these values are purely qualitative, in our case they directed us to choose these compounds for further investigations.

Conclusion

A structure-based pharmacophore model was generated and validated by establishing a means to correctly retrieve active AChE inhibitors from our self-compiled database of known synthetic inhibitors. In addition, accurate and reproducible retrieval of the AchE-inhibiting secondary plant metabolites that are complimentary to our natural product database was established. For example, secondary metabolites other than GNT could be found, e.g., coumarins from *Angelica gigas*[34] or zeatin, a derivate of purine adenine.[35] The coumarins SCT and SCN were obtained as promising AChE inhibiting hits from the in silico screening of the multiconformational 3D database NPD and successfully tested with respect to their anticholinesterase potential.

This is the first report where the in vivo ACh concentration with application of coumarins is investigated. The in vitro and in vivo results obtained from SCT and SCN strongly suggest that at least one path of their ability to alleviate the extracellular concentration of ACh in the nucleus accumbens may occur through inhibition of the AChE activity, as predicted in our elaborated pharmacophore model.

The relevance of coumarins for human risk assessment in terms of their metabolism, toxicity, and carcinogenicity was reviewed by Lake in 1999.[36] The mechanism of coumarin-induced tumor formation in rodents is associated with a 3,4-epoxidation pathway, resulting in the formation of toxic metabolites. In most human subjects, however, the 7-hydroxylation seems to be the major pathway of detoxification. It is concluded that the human exposure to coumarins from food and/or cosmetic products is harmless. Coumarins with a free position on C7 might be prodrugs, whereas the 7-hydroxycoumarins should act as active moieties, as reported for coumarin and 7-hydroxycoumarin.[37] The bioavailability of SCT might therefore be of high relevance upon oral administration. No information is available concerning the brain penetration of the more polar coumarin glucoside SCN or about a probable active transport system. Nevertheless, the determination of the AChE inhibitory activity was of high theoretical interest in this study because our model predicted a distinct interaction with all the generated features within the AChE pharmacophore model for both coumarins.

It is reported by Inestrosa and coauthors[9] that the AChE activity, responsible for acceleration of Aβ deposi-

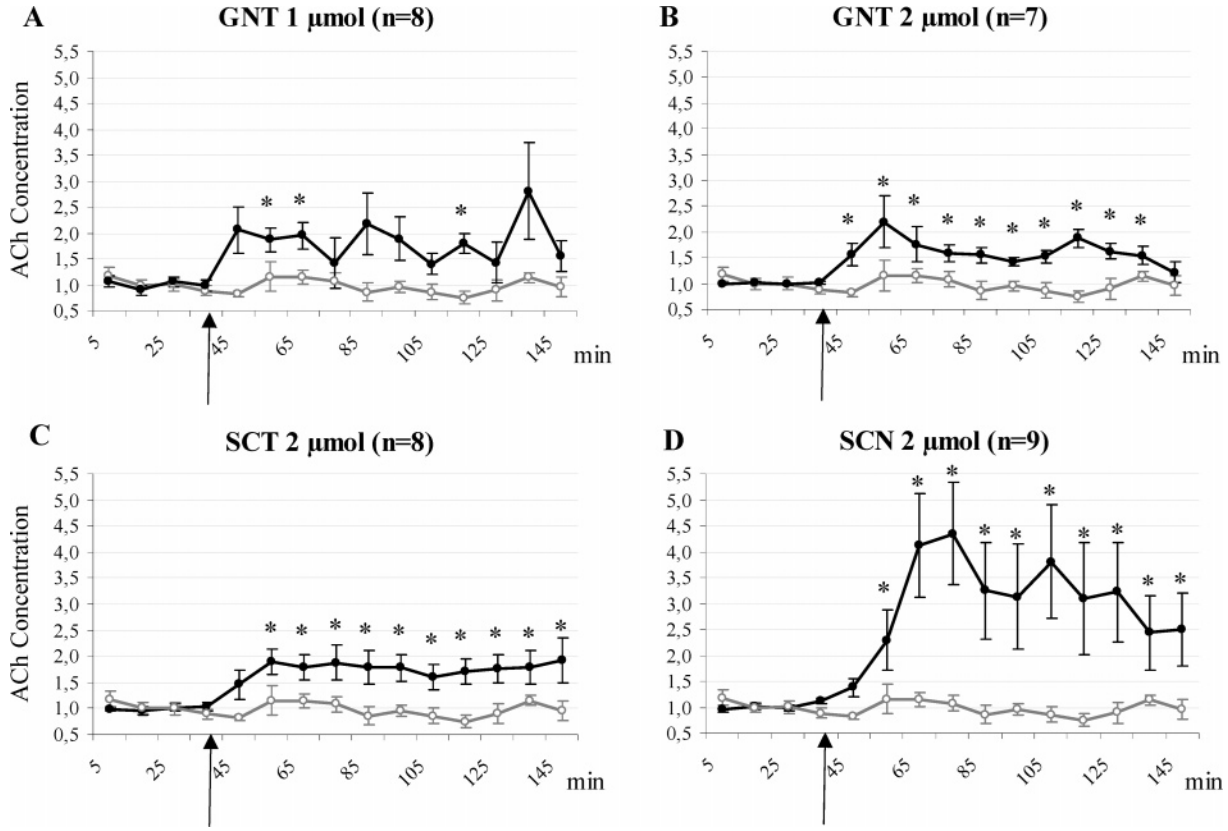

Figure 6. Effects of the drugs [depicted in black; (A) GNT, 1 μM; (B) GNT, 2 μM; (C) SCT, 2 μM; (D) SCT, 2 μM] on the extracellular concentration of ACh in the nucleus accumbens in comparison to the vehicle [DMSO−EtOH (1:1); depicted in gray; $n = 6$]. Arrows indicate time when icv injection (20 μL at 2 μL/min) was started. Data are relative values (means ± SEM). Four samples before the start of the injection were taken as controls (*$p < 0.05$, baseline samples vs the postinjection samples).

tion, is not affected by inhibitors binding at the enzyme's active site. It is suggested that peripheral binding site ligands are involved in Aβ formation. Another correlation with the development of Aβ plaques in AD patients seems to be associated with an increased monoamine oxidase B activity.[38] Therefore, compounds with inhibitory activity toward monoamine oxidase (mainly B) and AChE are suggested as useful in the treatment of AD. This dual inhibition could already be illustrated in vitro with a set of mainly 3,4,7-subtituted coumarin derivatives.[39] Since SCT is already described as a moderate monoamino oxidase inhibitor,[20] a combined mechanism of an elevated ACh concentration and a decrease of Aβ plaques may be assumed for SCT. If this supposition proves to be correct, SCT is worth further investigation as a potentially useful therapeutic agent for patients suffering from dementia. An in vivo study is in progress where the therapeutic opportunities of SCT and its ability to improve memory impairment are elucidated.

Experimental Section

Molecular Modeling. The molecular modeling calculations were accomplished on a SGI PowerChallenge XL workstation equipped with eight MIPS R8000 processors (175 MHz) running an Irix 6.5 operating system and the Catalyst software package (Catalyst Version 4.7, Accelrys Inc., San Diego, CA). The database mining, using the generated pharmacophore as a three-dimensional query, was executed on a Linux PC cluster. VS experiments were conducted within Catalyst with the elaborated model as search queries by applying the Fast Flexible Search option. Compounds present in the DNP were stored as three-dimensional structure models in multiconformational data format,[13] and an index was built according to the presence or absence of chemical features in the molecules. In the VS procedure, the index was searched for compounds fulfilling the requirements defined by the query pharmacophore. All molecules remaining were then fitted in each of their stored conformations by rigid rotation and translation in order to determine if the chemical features of the structures were able to map the requested functions of the pharmacophore model. A compound is considered to be a hit only if all functions of the pharmacophore model are mapped by defined functions of the respective molecule. The quality of the fit (fitting value) depends on two parameters: the weights assigned to the hypothesis features and how close the features in the molecule are to the centers of the corresponding location constraints in the pharmacophore hypothesis. In the present study, weights were set to a value of one for all features.

Chemistry. ^{1}H NMR spectra of SCT and SCN were recorded in DMSO-d_6 on a Bruker Avance 300 spectrometer. Their identification in the crude extract was accomplished by HPLC−DAD−MS (Hewlett-Packard HP-1050 liquid chromatograph equipped with a DAD-detector coupled with a Finnigan MAT SSQ 7000 mass spectrometer with Digital DEC 3000 data station) according to the method described by Ganzera and coauthors.[30] Column chromatography (CC) was performed using silica gel 60 (Merck, Darmstadt, Germany; 0.040−0.063 mm, 230−400 mesh) and Sephadex LH-20 (Merck, Darmstadt, Germany).

Plant Material. The underground parts of *S. carniolica* Jacq. were purchased from Alfred Galke GmbH, Gittelde, Austria. Voucher specimens (JR-20030624 A1) have been deposited in the Herbarium of the Department of Pharmacognosy, Institute of Pharmacy, University of Innsbruck, Austria.

Extraction and Isolation. The rhizomes of *S. carniolica* (202 g) were crushed to a coarse powder and extracted with 600 mL of methanol for 10 h in a Soxhlet extractor. Upon removal of solvent in vacuo, the methanolic extract yielded 32 g. This crude extract was suspended in CH_2Cl_2 and

fractionated by silica gel flash column chromatography (5 × 35 cm) using a step-gradient of CH_2Cl_2–MeOH (CH_2Cl_2; CH_2Cl_2–MeOH 99:1, 98:2, 95:5, 90:10, 75:25, 60:40, 35:65; MeOH; 500 mL each) to give 14 fractions (A 1–14). Fractions A 5/6 (650 mg) and fraction A 10 (300 mg) contained fluorescent spots at 366 nm on silica gel TLC plates $60F_{254}$ (Merck, Darmstadt, Germany; developed in ethyl acetate/acetic acid anhydride/formic acid/water, 100:11:11:260) indicating a coumarin content. Both fractions were further purified by Sephadex CC (2 × 100 cm) with methanol to yield 51 mg of SCT and 87 mg of SCN, respectively. SCT and SCN were obtained from methanol as whitish needles and a white microcrystalline powder, respectively. Their physical and spectroscopic data are in good agreement with the literature.[30,40]

TLC and Microplate Test. The AChE inhibitory activity of the methanolic crude extract was qualitatively determined in a TLC assay using Ellman's method.[41] Additionally, a test to exclude false positive results was conducted as described by Rhee et al.[29] The silica gel TLC plates $60F_{254}$ (0.2 mm thickness) were purchased from Merck (Darmstadt, Germany). Ten microliters of the crude extract dissolved in methanol (10 mg/mL) and, as a reference substance, 10 μL of a solution of 100 μg and 10 μg of galathamine hydrobromide (GNT, purchased from Tocris, Cookson Ltd, Avonmounth, U.K.), respectively, were spotted on the TLC plate and developed in the solvent toluene–ether–methanol (1:1:2). Enzyme inhibitory activities were detected by spraying the substrate with dye and enzyme as described by Rhee and coauthors.[10]

SCT, SCN, and GNT were quantitatively tested by applying a modified Ellman's method in a 96-well microplate assay as described by Ingkaninan and coauthors.[31] In both test systems, the enzyme (acetylcholineesterase; Sigma-Aldrich Chemie Gmbh, Steinheim, Germany) hydrolyzes the substrate acetylthiocholine (acetylthiocholiniodid; Sigma-Aldrich Chemie Gmbh, Steinheim, Germany) to produce thiocholine. This reacts with Ellman's reagent [5,5′-dithiobis-(2-nitrobenzoic acid); Sigma-Aldrich Chemie Gmbh, Steinheim, Germany], resulting in 5-thio-2-nitrobenzoate and the yellow colored 2-nitrobenzoate-5-mercaptothiocholine, which was visually detected in the TLC test.

In the microplate assay, the absorbance of 2-nitrobenzoate-5-mercaptothiocholine was quantitatively measured at 405 nm with a Chameleon 5025 (Hidex, Finland) microplate reader at 0, 15, 30, 45, and 60 min after adding 25 μL of the 0.22 unit/mL AChE to the reaction mixture. The self-absorbance of all ingredients of the assay was corrected by subtracting the absorbance at time zero from the subsequent absorbance values. For the microplate assay, SCT and SCN were dissolved in DMSO to stock solutions of 100, 50, 25, 12.5, and 6.25 mM and diluted with a buffer (50 mM Tris-HCl, pH 8) at 1:100. Stock solutions of GNT in DMSO (10, 2.5, 0.625, 0.156, and 0.039 mM) were diluted with the buffer to give 100, 25, 6.25, 1.56, and 0.39 μM. The final concentration of DMSO in the microplate assay was 1%, to ensure that it did not disturb the test system. For all three substances the concentration dependence of their AChE inhibitory activity was determined. The percentage of the enzyme inhibition was calculated by comparing the rates for the sample to the blank (containing 1% DMSO) and analyzed with Student's *t*-test. The IC_{50} values were determined with Probit analysis. For statistical processing the SPSS 11.5 program package was used.

In Vivo Study. Surgery and Push–Pull Technique. Protocols of experiments were approved by the Bundesministerium für Wissenschaft, Forschung und Kunst, Austria, Kommission für Tierversuchsangelegenheiten. Sprague–Dawley rats (250–350 g) were anaesthetized with urethane at 1.2 g/kg, ip. The head was fixed in a stereotaxic frame and a push–pull cannula (outer tubing, o.d. 0.75 mm, i.d. 0.41 mm; inner tubing, o.d. 0.26 mm, i.d. 0.13 mm) was mounted on a microdrive. This was stereotaxically inserted through a hole in the skull into the nucleus accumbens (coordinates, mm from bregma: AP, +1.2; L, +2.5; V, −7.8).[42] A second hole was drilled into the skull for the icv application of drugs (coordinates, mm from bregma: AP, −2.8; L, +1.5) The nucleus accumbens was superfused at 20 μL/min with artificial cerebrospinal fluid (aCSF), pH 7.2, which consisted of 140 mmol L^{-1} NaCl, 3 mmol L^{-1} KCl, 1.2 mmol L^{-1} $CaCl_2$, 1 mmol L^{-1} $MgCl_2$, 1 mmol L^{-1} Na_2HPO_4, 0.3 mmol L^{-1} NaH_2PO_4, 3 mmol L^{-1} glucose, and 1 μmol L^{-1} neostigmine. One hour after the cannula insertion, the samples were collected into tubes kept at −20 °C in time periods of 10 min and then stored at −80 °C until acetylcholine (ACh) was determined.

Application of Drugs. GNT was dissolved in 20 μL of DMSO, and the coumarins were dissolved in DMSO–EtOH (1:1). Using a motorized microsyringe connected to a stereotaxic microdrive, the tip was introduced with an angle of 60° through the drug application hole into the ipsilateral ventricle (coordinates mm from bregma: AP, −0.9; L, +1.5; V, −3.8) via a cannula (o.d., 0.65; i.d., 0.38). The drug solutions were injected at 2 μL/min. The control rats were injected with the vehicle DMSO–EtOH (1:1).

Histology. At the end of the experiment, the rat was euthanized with an overdose of urethane, and the brain was removed and stored in buffered formaldehyde solution (7%). Serial coronal sections were cut at 50 μm intervals. Localization of the push–pull cannula and icv microinjection was verified. Experiments with unsatisfactory localization were discarded.

Determination of Acetylcholine (ACh). ACh content in the samples was determined by HPLC with a cation-exchange analytical column and a postcolumn reactor followed by electrochemical detection.[43,44] The system consisted of a HPLC-pump (JASCO PU-1580, Jasco Corp., Tokyo, Japan), a pulse dampener, and an autosampler (AS-4000, Hitachi Ltd., Tokyo, Japan) with a 100-μL sample loop. The mobile phase was 100 mM K_2HPO_4, 5 mM KCl, 1 mM tetramethylammonium hydroxide, 0.1 mM Na-EDTA, and 0.5 mL/L Kathon CG (Rohm & Haas, Frankfurt/Main, Germany), with the pH being adjusted to 7.9 with H_3PO_4. The mobile phase was pumped at a flow rate of 0.4 mL/min. ACh was separated on an analytical column (80 × 3 mm, Kromasil 100-5 C18) loaded with lauryl sulfate. At the postcolumn enzyme reactor (20 × 1 mm Kromasil 100-10 NH_2) to which AChE (Sigma-Aldrich Chemie, Steinheim, Germany) and choline oxidase (Sigma-Aldrich Chemie, Steinheim, Germany) were bound, ACh was hydrolyzed to acetate and choline. Subsequently, choline was oxidized to betaine and hydrogen peroxide. The peroxide was electrochemically detected by a UniJet platin electrode (3 mm) at +500 mV with an amperometric detector (BAS LC-4, Bioanalytical Systems, West Lafayette, IN). The detection limit for ACh (signal-to-noise ratio = 3) was 10 fmol per sample. ACh was quantified with external standards that were injected at the beginning and the end of the analysis.

Statistical significance of drug effects on ACh release was calculated by Friedman's analysis of variance, followed by Wilcoxon's signed rank test for paired data (*$p < 0.05$, **$p < 0.001$) using the mean release rate before the administration of drugs as controls. Data are shown as means ± SEM of relative values. The mean release rate before drug administration was taken as 1.0.

Acknowledgment. The authors thank Dr. Ernst P. Ellmerer (Institute of Organic Chemistry) for NMR measurements, Dr. Sonja Sturm (Institute of Pharmacy) for HPLC–MS measurements, and Gospava Stojanovic, Jasmin Aldrian, and Barbara Bergner (Innsbruck, Austria) for their excellent technical assistance.

References

(1) Newman, D. J.; Cragg, G. M.; Snader, K. M. Natural Products as sources of new drugs over the period 1981–2002. *J. Nat. Prod.* **2003**, *66*, 1022–1037.
(2) Brewer, S. The relationship between natural products and synthetic chemistry in the discovery process. *Chem. Soc. Spec. Pub.* **2000**, *257*, 59–65.
(3) Howes, M.-J. R.; Houghton, P. J. Plants used in Chinese and Indian traditional medicine for improvement of memory and cognitive function. *Pharmacol. Biochem. Behav*. **2003**, *75* (3), 513–527.

(4) Perry, E. K.; Pickering, A. T.; Wang, W. W.; Houghton, P. J.; Perry, N. S. L. Medicinal plants and Alzheimer's disease: From ethnobotany to phytotherapy. *J. Pharm. Pharmacol*. **1999**, *51*, 527−534.
(5) Roberson, M. R.; Harrell, L. E. Cholinergic activity and amyloid precursor protein metabolism. *Brain Res. Rev.* **1997**, *25*, 50−69.
(6) Bartus, R. T.; Dean, R. L.; Beer, B.; Lippa, A. S. The cholinergic hypothesis of geriatric memory dysfunction. *Science* **1982**, *217*, 408−414.
(7) Benzi, G.; Moretti, A. Is there a rationale for the use of acetylcholinesterase inhibitors in the therapy of Alzheimer's disease? *Eur. J. Pharmacol.* **1998**, *346*, 1−13.
(8) Selkoe, D. J. Amyloid β-protein and the genetics of Alzheimer's disease. *J. Biol. Chem.* **1996**, *271*, 18295−18298.
(9) Inestrosa, N. C.; Alvarez, A.; Perez, C. A.; Moreno, R. D.; Vicente, M.; Linker, C.; Casanueva, O. I.; Soto, C.; Garrido, J. Acetylcholinesterase accelerates assembly of amyloid-β-peptides into Alzheimer's fibrils: Possible role of the peripheral site of the enzyme. *Neuron* **1996**, *16*, 881−891.
(10) Rhee, I. K.; van de Meent, M.; Ingkaninan, K.; Verpoorte, R. Screening for acetylcholinesterase inhibitors from Amaryllidaceae using silica gel thin-layer chromatography in combination with bioactivity staining. *J. Chromatogr. A* **2001**, *915*, 217−223.
(11) Thomsen, T.; Kewitz, H. Selective inhibition of human acetylcholinesterase by galanthamine in vitro and in vivo. *Life Sci.* **1990**, *46*, 1553−8.
(12) Langer, T.; Krovat, E. M. Chemical feature-based pharmacophores and virtual library screening for discovery of new leads. *Curr. Opin. Drug Discovery Dev*. **2003**, *6*, 370−376.
(13) Rollinger, J. M.; Haupt, S.; Stuppner, H.; Langer, T. Combining ethnopharmacology and virtual screening for lead structure discovery: COX-inhibitors as application example. *J. Chem. Inf. Comput. Sci*. **2004**, *44*, 480−488.
(14) Muschietti, L.; Gorzalczany, S.; Ferraro, G.; Acevedo, C.; Martino, V. Phenolic compounds with antiinflammatory activity from *Eupatorium buniifolium*. *Planta Med.* **2001**, *67*, 743−744.
(15) Calixto, J. B.; Otuki, M. F.; Santos, A. R. Antiinflammatory compounds of plant origin. Part I. Action on arachidonic acid pathway, nitric oxide and nuclear factor kappa B (NF-kappaB). *Planta Med*. **2003**, *69*, 973−983.
(16) Fujioka, T.; Furumi, K.; Fujii, H.; Okabe, H.; Mihashi, K.; Nakano, Y.; Matsunaga, H.; Katano, M.; Mori, M. Antiproliferative constituents from umbelliferae plants. V. A new furanocoumarin and falcarindiol furanocoumarin ethers from the root of *Angelica japonica*. *Chem. Pharm. Bull.* **1999**, *47*, 96−100.
(17) Kim, N. Y.; Pae, H. O.; Ko, Y. S.; Yoo, J. C.; Choi, B. M.; Jun, C. D.; Chung, H. T.; Inagaki, M.; Higuchi, R.; Kim, Y. C. *in vitro* inducible nitric oxide synthesis inhibitory active constituents from *Fraxinus rhynchophylla*. *Planta Med*. **1999**, *65*, 656−658.
(18) Kang, T. H.; Pae, H. O.; Jeong, S. J.; Yoo, J. C.; Choi, B. M.; Jun, C. D.; Chung, H. T.; Miyamoto, T.; Higuchi, R.; Kim, Y. C. Scopoletin: An inducible nitric oxide synthesis inhibitory active constituent from *Artemisia feddei*. *Planta Med*. **1999**, *65*, 400−403.
(19) Farah, M. H.; Samuelsson, G. Pharmacologically active phenylpropanoids from *Senra incana*. *Planta Med*. **1992**, *58*, 14−18.
(20) Yun, B. S.; Lee, I. K.; Ryoo, I. J.; Yoo, I. D. Coumarins with monoamine oxidase inhibitory activity and antioxidative coumarino-lignans from *Hibiscus syriacus*. *J. Nat. Prod.* **2001**, *64*, 1238−1240.
(21) Shaw, C. Y.; Chen, C. H.; Hsu, C. C.; Chen, C. C.; Tsai, Y. C. Antioxidant properties of scopoletin isolated from *Sinomonium acutum*. *Phytother. Res*. **2003**, *17*, 823−825.
(22) Toda, S. Inhibitory effects of phenylpropanoid metabolites on copper-induced protein oxidative modification of mice brain homogenate, in vitro. *Biol. Trace Elem. Res*. **2002**, *85*, 183−188.
(23) Berman, H. M.; Westbrook, J.; Feng, Z.; Gilliland, G.; Bhat, T. N.; Weissig, H.; Shindyalov, I. N.; Bourne, P. E. The protein data bank. *Nucleic Acids Res.* **2000**, *28*, 235−242 (available online at www.rcsb.org/pdb/).
(24) LigandScout: This software package is available from Inte:Ligand GmbH, A-2344 Maria Enzersdorf, Austria (www.inteligand.com). Details and application are described: (a) Wolber, G.; Langer, T. LigandScout: 3D pharmacophores derived from protein-bound ligands and their use as virtual screening filters. *J. Chem. Inf. Comput. Sci.* **2004**, in press. (b) Langer, T.; Wolber; G. Virtual combinatorial chemistry and in silico screening: Efficient tools for lead structure discovery? *Pure Appl. Chem.* **2004**, *76*, 991−998.
(25) Harel, M.; Schalk, I.; Ehret-Sabatier, L.; Bouet, F.; Goeldner, M.; Hirth, C.; Axelsen, P. H.; Silman, I.; Sussman, J. L. Quaternary ligand binding to aromatic residues in the active-site gorge of acetylcholinesterase. *Proc. Natl. Acad. Sci. U.S.A.* **1993**, *90*, 9031−9035.
(26) Bartolucci, C.; Perola, E.; Pilger, C.; Fels, G.; Lamba, D. Three-dimensional structure of a complex of galanthamine (nivalin) with acetylcholinesterase from *Torpedo californica*: Implications for the design of new anti-Alzheimer drugs. *Proteins* **2001**, *42*, 182−191.
(27) Wagner, H.; Bladt, S.; Zgainski, E. M. *Drogenanalyse, Dünnschicht-chromatographische Analyse von Arzneidrogen*; Springer-Verlag: Berlin, 1983; pp 145−161.
(28) Nowak, S.; Dzido, T. H.; Soczewinski, E.; Wolbis, M. Quantitative determination of coumarins, flavonoids and chlorogenic acid in the leaves and underground parts of some species of genus *Scopolia* Jacq. *Acta Pol. Pharm*. **2002**, *59* (4), 259−263.
(29) Rhee, K.; van Rijn, R. M.; Verpoorte, R. Qualitative determination of false-positive effects in the acetylcholinesterase assay using thin-layer chromatography. *Phytochem. Anal.* **2003**, *14*, 127−131.
(30) Ganzera, M.; Sturm, S.; Stuppner, H. HPLC-MS and MECC analysis of coumarins. *Chromatographia* **1997**, *46*, 197−203.
(31) Ingkaninan, K.; de Best, C. M.; van der Heijeden, R.; Hofte, A. J. P.; Karabatak, B.; Irth, H.; van der Greef, J.; Verpoorte, R. High-performance liquid chromatography with on-line coupled UV, mass spectrometric and biochemical detection for identification of acetylcholinesterase inhibitors from natural products. *J. Chromatogr. A* **2000**, *872*, 61−73.
(32) Lopez, S.; Bastida, J.; Viladomat, F.; Codina, C. Acetylcholinesterase inhibitory activity of some Amaryllidaceae alkaloids and Narcissus extracts. *Life Sci.* **2002**, *71*, 2521−2529.
(33) Bores, G. M.; Huger, F. P.; Petko, W.; Mutlib, A. E.; Camacho, F.; Rush, D. K.; Selk, D. E.; Wolf, V.; Kosley, R. W., Jr.; Davis, L.; Vargas, H. M. Pharmacological evaluation of novel Alzheimer's disease therapeutics: Acetylcholinesterase inhibitors related to galanthamine. *J. Pharmacol. Exp. Ther*. **1996**, *277*, 728−738.
(34) Kang, S. Y.; Lee, K. Y.; Sung, S. H.; Park, M. J.; Kim, Y. C. Coumarins isolated from *Angelica gigas* inhibit acetylcholinesterase: Structure−activity relationships. *J. Nat. Prod*. **2001**, *64*, 683−685.
(35) Heo, H.-J.; Hong, S.-C.; Cho, H.-Y.; Hong, B.; Kim, H.-K.; Kim, E.-K.; Shin, D.-H. Inhibitory effect of zeatin, isolated from *Fiatoua villosa*, on acetylcholinesterase activity from PC12 cells. *Mol. Cells* **2002**, *13*, 113−117.
(36) Lake, B. G. Coumarin metabolism, toxicity and carcinogenicity: Relevance for human risk assessment. *Food Chem. Toxicol*. **1999**, *37*, 423−453.
(37) Ritschel; W. A.; Hoffmann, K. A. Pilot study on bioavailability of coumarin and 7-hydroxycoumarin upon peroral administration of coumarin in a sustained-release dosage form. *J. Clin. Pharmacol.* **1981**, *21*, 294−300.
(38) Saura, J.; Luque, J. M.; Cesura, A. M.; Da Prada, M.; Chan-Palay, V.; Huber, G.; Loffler, J.; Richards, J. G. Increased monoamine oxidase B activity in plaque-associated astrocytes of Alzheimer brains revealed by quantitative enzyme radioautography. *Neuroscience* **1994**, *62*, 15−30.
(39) Bruehlmann, C.; Ooms, F.; Carrupt, P.-A.; Testa, B.; Catto, M.; Leonetti, F.; Altomare, C.; Carotti, A. Coumarins derivatives as dual inhibitors of acetylcholinesterase and monoamine oxidase. *J. Med. Chem*. **2001**, *44* (19), 3195−3198.
(40) Wolbiœ, M.; Nowak, S. Coumarins and phenolic acids from the underground part of *Scopolia lurida* Dun. *Acta Pol. Pharm.* **1994**, *51*, 171−174.
(41) Ellman, G. L.; Courtney, D.; Andres, V., Jr.; Featherstone, R. M. A new rapid calorimetric determination of acetylcholinesterase activity *Biochem. Pharmacol*. **1961**, *7*, 88−95.
(42) Paxinos, G.; Watson, H. *The rat brain in stereotaxic coordinates*, 4th ed.; Academic Press: Sidney, 1998.
(43) Damsma, C.; Westerink, B. H. C.; Imperato, A.; Rollema, H.; De Vries, J. B.; Horn, A. S. Automated brain dialysis of acetylcholine in freely moving rats: Detection of basal acetylcholine. *Life Sci*. **1987**, 873−876.
(44) Prast, H.; Tran, M. H.; Fischer, H.; Philippu, A. Nitric Oxide-induced release of acetylcholine in the nucleus accumbens: Role of cyclic GMP, glutamate, and GABA. *J. Neurochem.* **1998**, *71*, 266−273.

JM049655R